Biosensors and Bioelectronics 128 (2019) 122–128

Contents lists available at ScienceDirect

Biosensors and Bioelectronics

journal homepage: www.elsevier.com/locate/bios

Picomolar detection of retinol binding protein 4 for early management of type II diabetes

Anirban Paul[a,b], Maria Serena Chiriacò[c], Elisabetta Primiceri[c], Divesh N. Srivastava[a,b,*], Giuseppe Maruccio[c,d,**]

[a] Analytical & Environmental Science Division and Centralized Instrument Facility, CSIR-Central Salt and Marine Chemicals Research Institute (CSMCRI), Gijubhai Badheka Marg, Bhavnagar 364002, Gujarat, India
[b] Academy of Scientific and Innovative Research (AcSIR), Ghaziabad 201002, India
[c] CNR NANOTEC Institute of Nanotechnology, via Monteroni, 73100 Lecce, Italy
[d] Department of Mathematics and Physics, University of Salento, via Monteroni, 73100 Lecce, Italy

ARTICLE INFO

Keywords:
Retinol binding protein 4
Self-assembled monolayer
Impedance spectroscopy
Picomolar detection

ABSTRACT

Type (II) diabetes is one of the major threats to mankind as it causes insulin resistance in human body and Retinol Binding Protein 4 (RBP4) is currently considered as a potential biomarker for early management of this disease. Hence a low-level detection of RBP4 is a very important task and for this purpose, a novel RBP4 biosensor has been developed using homemade plastic chip electrodes (PCEs) as a platform for self-assembled monolayer (SAM) of 4-ATP and further functionalization with glutaraldehyde. Anti RBP4 is used as biorecognition species and electrochemical impedance spectroscopy has been performed to detect different RBP4 concentrations plotted against charge transfer resistance. A wide concentration range from 100 fg/mL to 1 ng/mL has been tested and a low limit of detection (LOD) of 100 fg/mL has been achieved. This is the first report for fabrication of electrochemical biosensor of RBP4 using Ag-Ab interaction having such low LOD. The sensor is characterized by various physico-chemical techniques. Excellent reproducibility and quick measurement make this biosensor extremely useful for the biomedical industry.

1. Introduction

Type 2 diabetes (T2D) is currently known to be one of the most challenging health problems worldwide and hence a major threat to mankind. The disease is mainly characterized by the inability of the cells to receive insulin hormone inducing insulin resistance (García-Jiménez et al., 2016). The reasons behind such insulin resistance include genetics, physical inactivity, obesity, diet, medical treatments, environmental toxicants, stress, and endocrine disturbances. Among them, obesity is considered to be one of the most and major factors which directly affects secretion of insulin and lead to T2D (Hodjat et al., 2017; Johnson and Olefsky, 2013; Khan et al., 2017; Mostafalou et al., 2012; Pakzad et al., 2013). The most alarming issue with diabetes is that complications appear far after the early stages of the disease, in a quite mature stage, in which glucose tolerance barrier is weakened and the patient become diabetic. Diabetes is not only a problem for those suffering from this disease but it is also a big issue for public health as billions of dollars are spent annually to prevent or take care of such pathology, but till now no permanent solution has been suggested and hence diabetic patients are advised to constantly monitor their blood glucose level and take insulin shots periodically to maintain their normal blood glucose level (Farshchi et al., 2014; Nichols et al., 2016). Hence prognosis or pre-management of T2D is an extremely necessary task as it would not only reduce the chances of becoming diabetic but would also save a huge amount of money and effort. (Narayan et al., 2011) Several studies have been conducted in the management of diabetes, such as administration of antioxidants (Rahimi et al., 2005; Tabatabaei-Malazy et al., 2013), development of new drugs, transplantation of isolated insulin producing cells, and clinical practice guidelines (Avouris, 2010; Tabatabaei-Malazy et al., 2016; Vakhshiteh et al., 2013). Multiple laboratory tests are used for the diagnosis and management of patients with T2D. The blood glucose concentration and glycated Hemoglobin A1c (HbA1c) are the major diagnostic criteria for T2D monitoring. It has long been known that more than 50 genes are

* Corresponding author at: Analytical & Environmental Science Division and Centralized Instrument Facility, CSIR-Central Salt and Marine Chemicals Research Institute (CSMCRI), Gijubhai Badheka Marg, Bhavnagar 364002, Gujarat, India.
** Corresponding author at: CNR NANOTEC Institute of Nanotechnology, via Monteroni, 73100 Lecce, Italy.
E-mail addresses: dnsrivastava@csmcri.res.in (D.N. Srivastava), giuseppe.maruccio@unisalento.it (G. Maruccio).

https://doi.org/10.1016/j.bios.2018.12.032
Received 10 November 2018; Received in revised form 14 December 2018; Accepted 18 December 2018
Available online 24 December 2018
0956-5663/ © 2018 Elsevier B.V. All rights reserved.

involved in metabolic pathways related to pancreatic β cell, insulin functions, glucose metabolism, or any other circumstances that enhance the risk of T2D and these genes have also a predictive role in disease development. Adipose tissue is considered to be one of the important organs which regulate glucose and lipid in our body by secreting adipokines, a particular class of communication molecules. It is clinically proved that obesity prevents normal secretion of adipokines leading to dysregulation of insulin secretion which ultimately leads to T2D. Among several other adipokines, recently Retinol binding protein 4 (RBP4), a 201 amino acid peptide, has gained consideration as an excellent marker for T2D. RBP4 binds specifically with retinol and transports it in the blood stream to the liver. Elevated serum levels of RBP4 have been found in insulin-resistant mice and humans with obesity and type 2 diabetes (Yang et al., 2005) causing dysfunctions in the production of glucose transporter 4 and ultimately leading to failure of glucose uptake from blood.

The commonly available protein biomarker-based approaches utilized for the detection of T2D include enzyme-linked immunosorbent assay (ELISA) (Cork et al., 2013; Lee et al., 2018), Western blot (Mahmood and Yang, 2012), enzyme immunoassay (EIA) (Fernández-Sánchez et al., 2004), radioimmunoassay and mass spectrometry (Hirtz et al., 2016). However, these techniques are affected by a number of limitations such as availability, complexity, the requirement of heavy benchtop instruments and skilled personnel, costly materials, and long time of analysis (Cork et al., 2013; Parkash and Shueb, 2015). Conventionally, RBP4 in serum is detected by antibody-based assays such as ELISA (sandwich/competitive) (Brazaca et al., 2016). However, western blot analysis is the most reliable and superior method for monitoring RBP4 levels (Lee et al., 2016). This method is not rapid and requires a large number of samples for analysis. Innovative biosensors can solve some of these issues detecting targets via biochemical reactions and taking advantage of transducers able to convert biological or chemical reactions to electrical, thermal, or optical signals. These systems offer some advantages such as rapid detection, portability and patient flexibility (Hassani et al., 2018; Okafor et al., 2014). Some innovative methods have been reported for the detection of RBP4 in serum samples, like a novel aptamer-based Surface Plasmon Resonance (SPR) biosensor (Lee et al., 2012), in which a gold chip was functionalized with RBP4-specific and used for SPR-based label-free detection of RBP4. The minimum limit of detection of the biosensor was 75 nM (1.58 μg/mL) RBP4. Lee et al. developed an enzyme-linked antibody-ssDNA aptamer sandwich (ELAAS) method to detect RBP4 (Lee et al., 2008). There are reports for detection of RBP4 using DNA immunation and mass spectrometry immunoassay (Bian et al., 2010; Kiernan et al., 2011). All these reported methods require sophisticated and costly analytical instrumentations for sample pretreatment and measurements which affect the utility of the biosensor for field use. Thus, there is a need for the development of new biosensors with lower detection limits and simple transduction mechanisms for easier handling and point of care applications.

Capacitive and impedimetric immunosensors exploit the change in dielectric properties due to the change in thickness of the dielectric layer at the electrolyte-electrode interface, resulting from the antibody-antigen interaction process. McNeil et al. (Fernández-Sánchez et al., 2004) reported impedimetric prostate specific antigen (PSA) immunosensor based on the lateral flow assay format, Mustafa et al. (Sonuç and Sezgintürk, 2014) developed an ultrasensitive impedimetric immunosensor for HER3. Our group also successfully exploited the sensing principle to fabricate impedometric sensors for various biomarkers. (Chiriacò et al., 2013a, 2013b, 2015, 2018). One of the important components for fabrication of impedometric sensor is the electrode. Carbon or Au screen printed surface, ITO coated the surface or glassy carbon electrodes are popularly used in this regard (Canbaz and Sezgintürk, 2014). Here in this manuscript, we propose Plastic Chip Electrode (PCE) as working electrode for performing inexpensive immunoassays for picomolar detection of RBP4. PCE is a polymer composite electrode made up of graphite and polymethylmethacrylate. Unlike the screen printed electrode which is very popular in point-of-care devices, the PCE is less prone to damage as its conductive layer is not just a coating over a substrate but an integral part of it. It's fabrication and characterization had already been reported earlier. (Perween et al., 2014) We have successfully used this electrode for multiple applications like electrocatalysis, electrometallurgy and anodic stripping voltammetry etc. (Perween and Srivastava, 2017) In this work, anti-RBP4 has been functionalized on PCE in the form of self-assembled monolayers, which allow the immobilization of biomolecules in a very specific and reproducible pattern (Nuzzo and Allara, 1983; Barrett et al., 2005; Han et al., 2010; Li et al., 2007; Patil et al., 2014; Wen et al., 2013). In particular, 4-ATP was employed as a bridge between chemical and biological interfaces since its thiol termini bind strongly with gold on one side while its -OH terminal chemically binds -CHO terminal of glutaraldehyde (GA) on the other. The two termini of GA consist of aldehyde which acts as a channel as one terminal is bound to 4-ATP whereas the other terminal will bind amino terminal of protein. The reaction is generally carried out in a dark environment (Sonuç and Sezgintürk, 2014). The concentration of human RBP4 was estimated utilizing Antigen-Antibody (Ag-Ab) interaction by measuring charge transfer resistance in aqueous Fe(II)/Fe(III) solution. A low-level detection of 100 fg/mL was achieved for human RBP4. Various control experiments were carried out to verify the selectivity of the biosensing assay. This is the first report based on our knowledge for fabrication of RBP4 impedometric sensors with such low limit of detection. The wide concentration range, ease of operation and low detection limit make this RBP4 sensor superior compared to other reported biosensors for this protein.

2. Materials and methods

2.1. Materials

Graphite powder was purchased from CDH Pvt. Ltd. and poly (methyl methacrylate) (PMMA) was purchased from Otto Chemie Pvt. Ltd. and used without further purification. Bovine serum albumin (BSA), Tris hydrochloride (Tris-HCl) and Disodium hydrogen phosphate (Na_2HPO_4), 4-aminothiophenol (4-ATP) were purchased from Sigma-Aldrich. Human Retinol Binding Protein 4 (RBP4) (ab59967), Recombinant Human Vaspin protein (ab86032) and Retinol-Binding Protein 4 monoclonal antibody (RBP4 mAb) (ab109193) were purchased from Abcam USA and used without further purification. Immunoglobin G protein has been purchased in pure form from Sigma-Aldrich whereas Glutaraldehyde (GA) was purchased from TCI Chemicals. Potassium ferrocyanide ($K_4Fe[CN]_6$) and potassium chloride (KCl) were purchased from SRL Chemicals, India. Potassium ferricyanide ($K_3Fe[CN]_6$), Potassium hydrogen phosphate (KH_2PO_4) and Sodium chloride (NaCl) were obtained from SISCO Research Laboratory Private Limited, Qualigens Fine Chemicals and Rankem respectively. EDTA was obtained from Alfa Aesar. Chloroform (Excel AR grade) was obtained from Fisher Scientific. High quality polyester sheets employed as the template in composite preparation were purchased from a local vendor.

2.2. Methods

2.2.1. Preparation of plastic chip electrodes

Plastic chip electrodes were fabricated through a previously reported method (Perween et al., 2014). A simple composite in 60:40 ratio of graphite and poly methyl methacrylate (PMMA) was taken in chloroform. The composite was stirred constantly with a glass rod and ultrasonicated for 15 min. A thick slurry of graphite-PMMA composite was poured into a specific template (10 cm × 10 cm glass plate) and dried overnight. The composite electrode was peeled out from the template and cut into pieces having a size of 3 cm × 0.8 cm

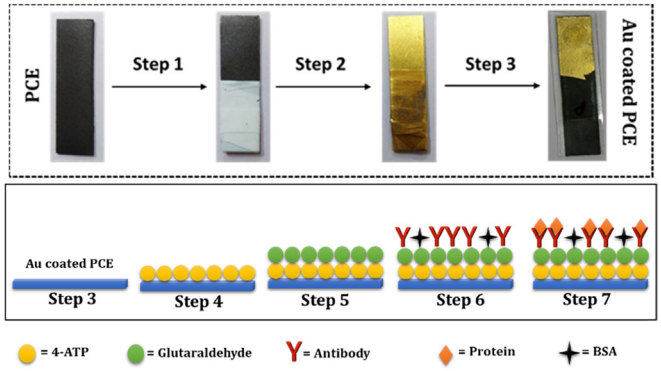

Scheme 1. Schematic diagram for stepwise functionalization of PCE for the fabrication of RBP4 biosensor.

(length × width).

2.2.2. Tailoring the surface of plastic chip electrodes

Gold electrodes are used regularly to obtain the immobilization of biomolecules via self-assembled monolayers of thiols. Therefore, we coated the working area of PCE with sputtered gold. The strategy is depicted in Scheme 1. Step 1 consists in wrapping the PCE with Teflon tape to avoid coating over an undesired area of the electrode. During Step 2, 10 nm of gold is deposited over PCE surface, using sputter coater. In Step 3, the teflon tape was removed and the PCE was laminated in the folds of a 120 μm plastic sheet by heat-press. A 5 mm diameter circle was pre-carved on the plastic sheet, using a precise plotter cutter, which makes the working area of the electrode identical. The sputter coated PCE was then functionalized in order to immobilize proteins. The fresh gold coated PCE was washed several times with milli-Q water and 10 μL of 0.1 M 4-aminothiophenol solution, prepared in ethanol, was drop-cast over the working area of Au coated PCE (step 4). The electrode was kept at room temperature for 12 h to form a self-assembled monolayer (SAM) on PCE. The surface-modified PCE was then washed thoroughly with milli-Q water and pretreated with 10 μL of Glutaraldehyde (GA) solution (2.5%). Next, the substrate was kept in dark environment to activate the amino-ends of 4-ATP (step 5). Then the surface modified electrode was washed with milli-Q water and dried under an argon stream at room temperature. Once the glutaraldehyde was dried, the tailored PCE was ready for antibody immobilization. 10 μL of 1 μg/mL of RBP4 antibody was deposited over the glutaraldehyde surface and the electrode was allowed to dry under room temperature for 6 h (step 6). The antibody modified electrode was then immersed into a 0.1% BSA solution to avoid any unspecific binding. The electrode was then washed several times with milli-Q water and stored at 4 °C for further use.

10 μL of Human RBP4 protein was prepared in PBS buffer, pH 7.4 and drop-cast over the antibody immobilized surface and the electrode was kept at room temperature for another 6 h (step 7). The functionalized electrode was dipped into 10 mM 1:1 Fe(II)/ Fe(III) solution, prepared in PBS, pH 7.4, for impedance measurements.

Surface morphology of PCE, before and after functionalization had been done by Field-Emission Scanning Electron Microscopy (FE-SEM) JEOL JSM 7100F and Attenuated total reflectance (ATR) spectral measurements of the functionalized probe had been carried out by Agilent Technology 600 series.

2.2.3. Electrochemical measurement

Electrochemical impedance spectroscopy measurements were performed using Princeton applied research potentiostat-galvanostat (PARSTAT 2273) by a three-electrode system. Modified PCE was used as working electrode, with a Pt foil used as counter electrode and Ag/AgCl (sat. KCl) as a reference electrode. The supporting electrolyte used for these measurements were 10 mM 1:1 $K_3Fe(CN)_6/K_4Fe(CN)_6$ in 0.1 M PBS (pH 7.4) buffer. The impedance spectra were collected within the frequency range of 100 kHz–0.1 Hz with 5 mV amplitude of the applied sine wave in open circuit condition. Nyquist plots were derived to get charge transfer resistance by fitting the impedance data with an equivalent circuit using Zsimp Win software (Version 3.21). Cyclic voltammetry was performed on the same setup used for impedance measurements.

3. Results and discussion

3.1. Physico chemical characterization of the sandwich immunoassay

To characterize the PCE surface morphology before and after protein functionalization, we have performed Field emission scanning electron microscopy (FE-SEM) on three different samples. The morphology of the bare plastic chip electrode is reported in Fig. S1 (A-D) (ESI). The low-resolution image shows a mostly irregular surface having multiple pores (A-B) while the high-resolution image shows solid creeks (C-D). After evaporation of the solvent, polymer plays the major role to act as a matrix and conceal the filler (graphite particles), making a percolating conducting channel, so that the composite shows bulk conductivity as a whole. The morphology of the gold coated PCE is depicted in Fig. S2**(A)** (ESI), whereas the electron dispersive X-Ray (EDX) mapping in Fig. S2**(B)** (ESI) indicates a uniform coverage of the PCE by gold (in red color) justifying them as an excellent alternative to screen printing. In Fig. S2**(C)** (ESI), the EDX metal peak distribution is also reported. The morphology was investigated after drop-casting 1 ng/mL solution of RBP4 protein over gold coated PCE and drying for 12 h at room temperature. The protein immobilized surface of a gold coated PCE was kept at 4 °C and FE-SEM was recorded in liquid nitrogen assisted cryo atmosphere. Results are reported in Fig. 1**(A)**. Hollow spherical vesicle-like structures of RBP4 protein were observed, with an average diameter of 125 nm. To confirm the presence of protein, we have performed elemental mapping analysis by focusing the electron beam on one of the spherical vessels and we obtained the presence of oxygen, carbon, sodium and nitrogen along with a high abundance of gold. The result is reported in Fig. 1**(B)**. Presence of sodium is due to the buffer and the remaining elements strongly suggest the presence of protein over gold coated PCE surface.

FT-IR spectra have been obtained to confirm the surface functionalization of Au coated PCE, which have been dipped in 0.1 M solution of 4-aminothiophenol for 12 h and dried for 3 h at room temperature and finally under argon gas flow. The self-assembled monolayer of 4-ATP was scanned under attenuated total reflection probe attached with FT-IR spectrometer and the FT-IR spectra were recorded. Results are shown in Fig. S3 (ESI). Standard peaks of ν(CN) at 1085 cm^{-1}, ν(CH) at 2927 cm^{-1} and $\nu(NH_2)$ at 3355 cm^{-1} confirm the surface functionalization of Au by 4-ATP (Stevens et al., 2017). These results support the backbone of sensory response as without surface functionalization, it is merely impossible to immobilize proteins over the electrode surface. The results also suggest the suitability of the tailored plastic chip electrode for biosensing applications.

3.2. Electrochemical characterization of sandwich immunoassay

Electrochemical impedance spectroscopy (EIS) is a powerful tool to perform immunoassays and estimate the sensor response. (Biswas and Lee, 2011; Walker and Rapley, 2008). To proceed with EIS, it is useful to check the faradaic regime and the effect of sandwich immunoassay on electron transfer. Therefore, we performed cyclic voltammetry measurements with three electrode setup in the potential range of 0–1V in 10 mM 1:1 Fe(II)/Fe(III) in 0.1 M PBS pH 7.4 buffer. Pt electrode was taken as counter electrode whereas Ag/AgCl (sat. KCl) was employed as a reference electrode. Three different sandwich immunoassay samples had been performed and the result is depicted in Fig. 2**(a)**. Faradaic CV spectra with two distinct redox peaks in the cathodic and anodic region

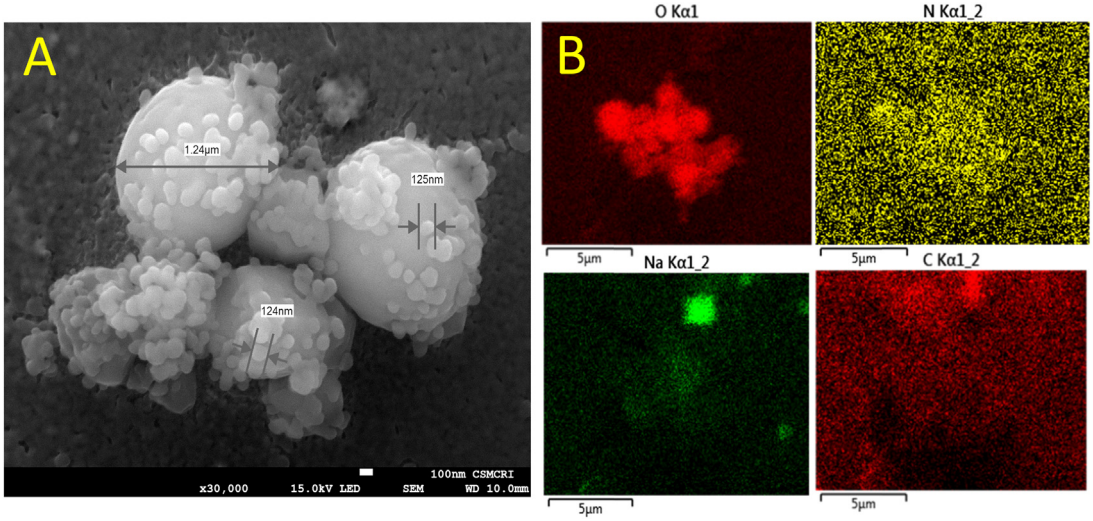

Fig. 1. (A) FE-SEM images of RBP4 protein decorated over gold coated PCE showing hollow spherical structure. (B) Elemental mapping of the hollow spherical microstructure to confirm the presence of protein over gold coated PCE surface.

were observed, describing the ease of electron transfer through the tailored electrode. The redox peaks spacing $\Delta E_p = (E_{pc} - E_{pa})$ was found to be 0.165 V for Au coated SAM-GA modified PCE (A), whereas $\Delta E_p = 0.263$ V for SAM-GA modified anti RBP4 (0.1 ng/mL) immobilized Au sputter coated PCE (B) and $\Delta E_p = 0.306$ V for RBP4 (0.1 ng/mL)-anti RBP4 (0.1 ng/mL) immobilized SAM-GA modified Au sputter coated PCE (C). The faradaic response was subsequently decreasing as the peak separation increases. This behavior can be ascribed to the increment in thickness of the biological species on the PCE surface, which inhibits the charge transfer resistance. The high intensity of the obtained current indicates that the tailored electrode is sufficiently conducting and charge transfer resistance can be monitored in a resistance domain in ohmic scale. The result also suggests that the functionalization protocol is working properly and can be implemented to measure biosensor response.

In the faradaic regime, molecular recognition on the electrode surface can be detected as a measurable change in the charge transfer resistance R_{ct}, which is directly related to the thickness of the functionalized layer. For this purpose, EIS measurements were carried out in a frequency range of 100 kHz-0.1 Hz using the same electrolyte solution employed for CV. The resulting Nyquist plots are reported in Fig. 2**(b)** and were fitted with an equivalent circuit $R_s[C_{dl}(R_{ct}W)]$ to extract the R_{ct} value, where R_s is related to solution resistance, C_{dl} corresponds to double-layer capacitance, and W is the Warburg impedance resulting from diffusion. R_{ct} is parallel with C_{dl} and in series with R_s. R_{ct} have been estimated for the three different conditions tested (A, B, C curves as described above) and it was found that R_{ct} increases from 62.8 Ω (ohms) for A to 98.6 Ω for B and 178.6 Ω for C. The increment of R_{ct} is related to the increment in thickness of the layers across electrode which alters transfer charge at the electrode/electrolyte interface and is also reflected in Nyquist plots.

3.3. Effect of Au sputter coating

Gold sputter coating has been deposited over the surface of plastic chip electrodes for two purposes. The first one is to increase the conductivity of PCE. The second is to exploit thiol chemistry to attach biomolecules on gold, resulting in an easier method compared to other functionalization techniques. The effect of sputter coating has been investigated by depositing two different gold thicknesses: 5 nm and 10 nm. The impedance spectra were collected in 10 mM 1:1 Fe(II)/Fe (III) solution in pH 7.4 PBS using Pt foil as a counter electrode and Ag/AgCl (sat. KCl) as a reference electrode in a frequency range from 100 kHz to 0.1 Hz. The obtained Nyquist plots are reported in Fig. S4 (ESI), where the impedance curve of bare PCE is compared with those corresponding to the two different gold thicknesses. R_{ct} of 10 nm thick Au coated PCE accounts for 58 Ω; this value is lower than $R_{ct} \approx 98$ Ω measured for around 5 nm thick Au coated PCE and both of them are much lower than R_{ct} associated to bare PCE (205 Ω). These results clearly point out the influence of the Au coating on EIS measurements. It can be argued that a thicker coating of gold can be effective but it will weaken the cause for the development of cheap sensing platform.

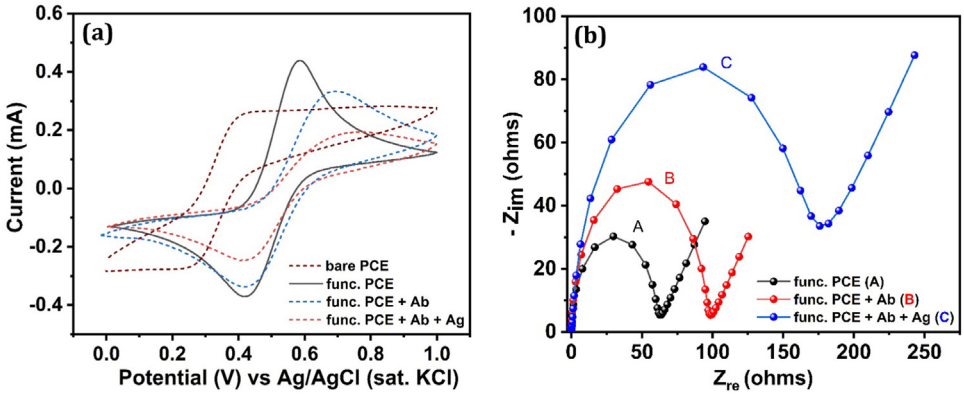

Fig. 2. (a). Cyclic voltammetry of bare PCE (brown dashed curve) Au coated SAM-GA modified PCE (black curve) SAM-GA modified PCE with anti-RBP4 (0.1 ng/mL) antibody immobilized Au (blue dashed curve) and RBP4 (0.1 ng/mL) on anti-RBP4 (0.1 ng/mL) Ab immobilized on SAM-GA modified PCE. (red dashed curve), **(b)**. Nyquist plot of (A - black curve) Au coated SAM-GA modified PCE (B - red curve) SAM-GA modified PCE with anti-RBP4 (0.1 ng/mL) antibody immobilized Au and (C - blue curve) RBP4 (0.1 ng/mL) on anti-RBP4 (0.1 ng/mL) Ab immobilized on SAM-GA modified PCE. (For interpretation of the references to color in this figure legend, the reader is referred to the web version of this article).

3.4. Effect of glutaraldehyde, BSA and other interferent proteins

Glutaraldehyde has a crucial role in the fabrication process of our biosensors as a crosslinker to bind protein molecules onto electrodes. In this respect, the SAM of 4-aminothiophenol has one terminal amino-group suitable for glutaraldehyde binding and crosslinking. However, glutaraldehyde may also hamper the biosensor activity. In order to establish how this could affect the biosensor response, we tested two different glutaraldehyde concentrations: 2.5% and 5% incubated over SAM-modified Au-coated PCE and we measured the impedance for both these conditions in the electrolyte solution. The corresponding Nyquist plots are reported in Fig. S5 **(ESI)** and indicate that 5% glutaraldehyde has a stronger effect on R_{ct}, as this parameter increases significantly with respect to immobilization with 2.5% glutaraldehyde and this is attributed to the formation of a thicker layer of glutaraldehyde. Hence 2.5% GA was chosen to be used in functionalization steps. We have also checked the change in the capacitive layer while blocking with BSA and the corresponding Nyquist plot is depicted in Fig. S6 (ESI). R_{ct} increases from 52.3 Ω to 83.3 Ω proving the formation of an insulating layer at the electrode-electrolyte interface. To check the viability of the sensor in a real environment, we have performed interference study with two proteins:IgG and Vaspin. All the three proteins have been taken at a same concentration of 0.5 pg/mL. The result is depicted in Fig. S7 **(ESI)** which suggests negligible interference due to selective recognition of an antigen-antibody pair of RBP4 which is ultimately responsible for the change in impedance.

3.5. Biosensor response to RBP4

For antibody immobilization, an RBP4 Ab solution (monoclonal antibody) was prepared in 10 mM PBS (8 g NaCl, 0.2 g KCl, 1.44 g Na_2HPO_4 and 0.24 g KH_2PO_4 in 1 L of sterile distilled water; pH 7.4). Then, 10 µL of RBP4 Ab solution (46.8 µg/mL) was added to the glutaraldehyde modified electrode. The electrode was then air-dried at room temperature, rinsed in PBS to remove any unbound antibodies and stored at 4 °C for further experiments. Various dilutions of RBP4 protein in the range of 0–25 pg/mL were prepared in PBS and 10 µL of each were added to the Ab-modified PCE surface. The electrode was air-dried for 1 h, followed by a washing step with PBS. Further, the modified electrode was rinsed in 0.1% BSA for blocking any unbounded site. The electrodes were rinsed again with PBS prior to electrochemical impedance measurements. The CV was performed with different RBP4 concentration solutions and the result is shown in Fig. 3**(a)**. The CV curves demonstrate a clear faradaic response with distinct redox peaks. If the anodic current is plotted with concentration, as in the inset of Fig. 3**(b)**, a linear response is obtained, proving that the fabricated electrodes can easily transfer charge and allow for further electrochemical impedance characterization. Biosensor response to RBP4 was measured by electrochemical impedance spectroscopy, using the functionalized electrodes immersed into 10 mM 1:1 Fe(II)/Fe(III) solution. Pt foil was used as counter electrode and Ag/AgCl (sat. KCl) as a reference electrode. The impedance was measured in a frequency domain

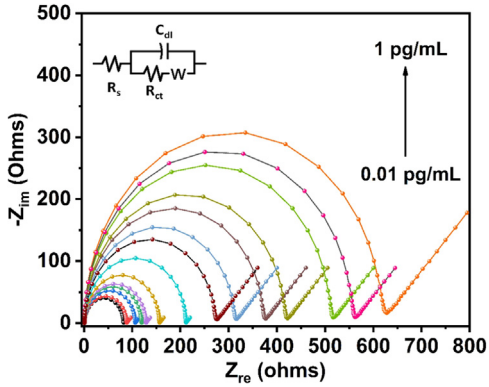

Fig. 4. Nyquist plots of RBP4 response at different concentrations in 1:1 Fe(II)/Fe(III) with tailored PCE as W.E., graphite rod as C.E. and Ag/AgCl (sat. KCl) as R.E. Input frequency domain 100 kHz–0.1 Hz. Plots were fitted with the circuit depicted in the inset.

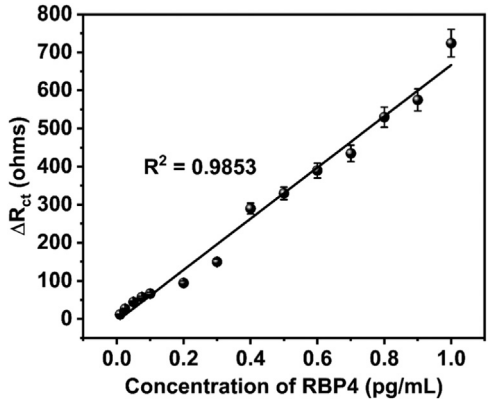

Fig. 5. Calibration plot of the RBP4 biosensor showing excellent linearity having a limit of detection of 0.01 pg/mL. (100 fg/mL).

of 100 kHz–0.1 Hz. Four concentrations (in the wide range from µg to fg) of RBP4 antigen were tested. Fig. 3**(b)** reports the resulting Nyquist plots. The R_{ct} for 1fg/mL is calculated to be 615.7 Ω; this value increases to 721.7 Ω for 1 pg/mL and to 2.6 kΩ for 1 ng/mL of RBP4 whereas the R_{ct} for 1 µg/mL concentration of RBP4 is calculated to be 3.42 kΩ. The gradual increase of R_{ct} proves that the functionalized electrode is extremely sensible in a wide range of concentrations and an fg/mL or pM detection limit can be achieved for RBP4.

3.6. Calibration plot

Obtaining a calibration plot is one the most important task in the development of a novel biosensor, as it gives information about its actual functionality and performance. For this purpose, after the

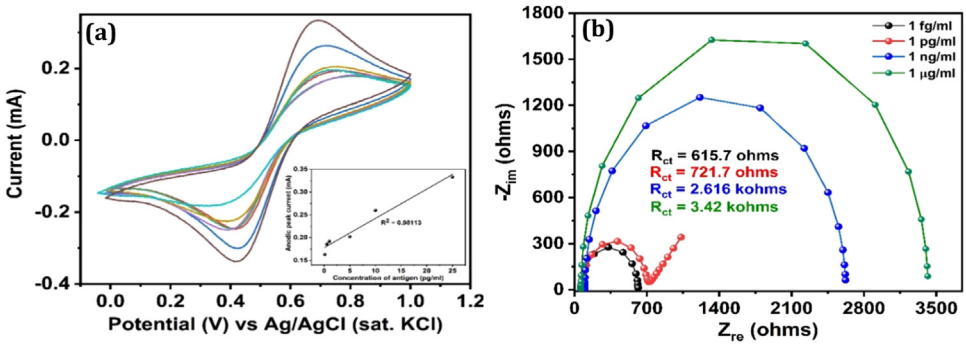

Fig. 3. (a) Cyclic voltammetry spectra of Ag-Ab interaction of RBP4 in SAM modified Au coated PCE showing a linear response in the anodic peak with a change of concentration (inset). (b) Nyquist plots of Ag-Ab interaction of RBP4 in SAM modified Au coated PCE show increment of ΔR_{ct} while increasing the concentration of RBP4.

Table 1
Comparative analytical performance of reported biosensors for RBP4.

Working principle	Linear range	LOD	References
enzyme-linked antibody-aptamer sandwich assays	0.2–5 μg/mL	78 ng/mL	Lee et al. (2012)
mouse IgA monoclonal antibody-based enzyme-linked immunosorbent sandwich assay	1–3 ng/mL	> 10 ng/mL	Lee et al. (2018)
ssDNA aptamer-based sandwich immunoassay using surface plasmon resonance	0.075–2 ng/mL	75 pg/mL	Lee et al. (2008)
Mass spectrometry RBP4 immunoassay	7.81–500 μg/mL	3.36 μg/mL	Pone et al.
DNA immunization RBP4 immunoassay	0.10–20 ng/mL	1 ng/mL	Bian et al.
Label free Impedometric sandwich immunoassay	**0.01–10^3** pg/mL	**100 fg/mL**	**This study**

optimization of tailored functionalization of PCE to detect low concentrations of RBP4, a narrow RBP4 concentration range was further considered employing 18 different dilutions from 0.01 pg/mL to 1 pg/mL. Impedance was measured applying standard experimental conditions discussed above. The experimental Nyquist plots are reported in Fig. 4 and show a gradual increase of the diameter of the semicircle, representing the R_{ct}, according to the growing concentration of RBP4. All curves were fitted with the $R_s[R_{ct}(C_{dl})Z_w]$ equivalent circuit to estimate the corresponding charge transfer resistances R_{ct} and R_{ct} of antiRBP4/BSA were then subtracted from R_{ct} of (anti RBP4/BSA/RBP4) to get ΔR_{ct} due to the variation of RBP4 concentration exclusively:

$$\Delta R_{ct} = R_{ct\ (antiRBP4/BSA/RBP4)} - R_{ct\ (antiRBP4/BSA)}$$

In Fig. 5, the obtained ΔR_{ct} are plotted as a function of concentration. The calibration plot of ΔR_{ct} and concentration has been repeated for 3 times and plotted with 5% error bar. The percentage of relative standard deviation was calculated as 1.3% of ΔR_{ct} for 13 consecutive dilutions, depicting the stability of the sandwich immunoassay. The result shows a linear increment with excellent adjacent R^2 of 0.96306 whereas Pearson's R is 0.9853 while the RBP4 detection limit is 100 fg/mL or 0.1 pg/mL. We have fitted the same calibration plot with some other function to get the goodness of fit. For this purpose, we have done logarithmic 3P1 plot and got a Pearson's R of 0.9626 and adjacent R^2 of 0.9559 with a reduced chi square of 12.815. The result shows more precision towards linear function rather than other functions.

The previous data demonstrate the good sensitivity in the low-detection limit. However, it is also important to get information on the dynamic range and its influence on the sensor response. For this reason, another calibration plot was obtained considering concentrations in the range from 50 pg/mL to 1 ng/mL and the corresponding Nyquist plots are fitted into the above-mentioned circuit and reported in Fig. S8 (ESI). Also in this case, Nyquist plots show the increasing of the semicircle with the increment of RBP4 concentration. In Fig. S9 (ESI), the calibration curve of concentration with charge transfer resistance shows a Langmuir type calibration with good R^2 demonstrating the effectiveness of the fabricated sensor in a large range of concentrations.

The comparison of the analytical performances of the label free impedometric immunosensor developed for RBP4 protein in this study with the other reported label free immunosensors for RBP4 in the pertinent literature is hereby reported (Table 1). The survey clearly suggests our result is superior to other reported methods in terms of wide range, limit of detection, reproducibility and ease of operation.

4. Conclusion

A highly sensitive and simple electrochemical disposable biosensor for the detection and quantification of RBP4 protein has been demonstrated in this study. Plastic chip electrodes with improved electronic conductivity thanks to the gold coated surface have been used to obtain a self-assembled monolayer of 4-ATP and glutaraldehyde as functionalization layer, able to bind antibody anti - RBP4 to the electrode surface. The sensor was able to detect RBP4 in the range from 100 fg/mL to 1 ng/mL. The R_{ct} values were found to be proportional to the concentration of RBP4 protein in the range of 0.01–1 pg/mL and from 50 pg/mL to 1 ng/mL. The limit of detection of the biosensor for RBP4 was as low as 100 fg/mL. To our knowledge, this is the first reported electrochemical impedometric biosensor for RBP4 with immobilized antibodies. The sensor also had better responses and lower limit of detection than the previously reported biosensors for RBP4. This is the first report for fabrication of impedometric sensor for detection of RBP4. Our developed biosensor has advantages of low costs, simple preparation and immobilization procedure, high selectivity and sensitivity, fast response, wide dynamic detection range and thanks to these features it has the potential to be largely used in the early detection and monitoring of type (II) diabetes.

CRediT authorship contribution statement

Anirban Paul: Conceptualization, Methodology, Software, Investigation, Data curation, Writing - original draft. **Maria Serena Chiriacò:** Software, Validation, Writing - review & editing. **Elisabetta Primiceri:** Investigation, Software, Resources, Writing - review & editing. **Divesh N. Srivastava:** Conceptualization, Methodology, Validation, Investigation, Writing - review & editing, Supervision, Project administration, Funding acquisition. **Giuseppe Maruccio:** Conceptualization, Validation, Investigation, Writing - review & editing, Supervision.

Acknowledgments

A.P. thanks CSIR, India for the Senior Research Fellowship (31/28(216)) and EMBO (ASTF 564-2016) for providing short-term fellowship to work at CNR, Lecce, Italy. This work was partially funded by the internal project (MLP-0018). Mr. Jibinlal A. and Miss Kirti are thankfully acknowledged for their help in carrying-out a few experiments. The CSIR-CSMCRI registration number: 187/2018.

Appendix A. Supporting information

Supplementary data associated with this article can be found in the online version at doi:10.1016/j.bios.2018.12.032.

References

Avouris, P., 2010. Nano Lett. 10, 4285–4294.
Barrett, D.A., Power, G.M., Hussain, M.A., Pitfield, I.D., Shaw, P.N., Davies, M.C., 2005. J. Sep. Sci. 28, 483–491.
Bian, C., Zhang, F., Wang, F., Ling, Z., Luo, M., Wu, H., Sun, Y., Li, J., Li, B., Zhu, J., Tang, L., Zhou, Y., Shi, Q., Ji, Y., Tian, L., Lin, G., Fan, Y., Wang, N., Sun, B., 2010. Acta Biochim. Biophys. Sin. 42, 847–853.
Biswas, C., Lee, Y.H., 2011. Adv. Funct. Mater. 21, 3806–3826.
Brazaca, L.C., Janegitz, B.C., Cancino-Bernardi, J., Zucolotto, V., 2016. ChemElectroChem 3, 1006–1011.
Canbaz, M.Ç., Sezgintürk, M.K., 2014. Anal. Biochem. 446, 9–18.
Chiriacò, M.S., de Feo, F., Primiceri, E., Monteduro, A.G., de Benedetto, G.E., Pennetta, A., Rinaldi, R., Maruccio, G., 2015. Talanta 142, 57–63.
Chiriacò, M.S., Luvisi, A., Primiceri, E., Sabella, E., De Bellis, L., Maruccio, G., 2018. Sci. Rep. 8 (7376), 1–8.
Chiriacò, M.S., Primiceri, E., Montanaro, A., de Feo, F., Leone, L., Rinaldi, R., Maruccio, G., 2013a. Analyst 138, 5404–5410.
Chiriacò, M.S., Primiceri, E., Monteduro, A.G., Bove, A., Leporatti, S., Capello, M., Ferri-Borgogno, S., Rinaldi, R., Novelli, F., Maruccio, G., 2013b. Lab Chip 13, 730–734.
Cork, J., Jones, R.M., Sawyer, J., 2013. J. Immunol. Methods 387, 140–146.
Farshchi, A., Esteghamati, A., Sari, A., Kebriaeezadeh, A., Abdollahi, M., Dorkoosh, F., Khamseh, M., Aghili, R., Keshtkar, A., Ebadi, M., 2014. J. Diabetes Metab. Disord. 13

(42), 1–14.
Fernández-Sánchez, C., McNeil, C.J., Rawson, K., Nilsson, O., 2004. Anal. Chem. 76, 5649–5656.
García-Jiménez, C., Gutiérrez-Salmerón, M., Chocarro-Calvo, A., García-Martinez, J.M., Castaño, A., De La Vieja, A., 2016. Br. J. Cancer 114, 716–722.
Han, M., Ishikawa, D., Honda, T., Ito, E., Hara, M., 2010. Chem. Commun. 46, 3598–3600.
Hassani, S., Maqbool, F., Salek-Maghsoudi, A., Rahmani, S., Shadboorestan, A., Nili-Ahmadabadi, A., Amini, M., Norouzi, P., Abdollahi, M., 2018. EXCLI J. 17, 57–71.
Hirtz, C., Vialaret, J., Gabelle, A., Nowak, N., Dauvilliers, Y., Lehmann, S., 2016. Sci. Rep. 6, 1–10.
Hodjat, M., Rahmani, S., Khan, F., Niaz, K., Navaei–Nigjeh, M., Mohammadi Nejad, S., Abdollahi, M., 2017. Arch. Toxicol. 91, 2577–2597.
Johnson, A.M.F., Olefsky, J.M., 2013. Cell 152, 673–684.
Khan, F., Momtaz, S., Niaz, K., Hassan, F.I., Abdollahi, M., 2017. Food Chem. Toxicol. 107, 406–417.
Kiernan, U.A., Phillips, D.A., Trenchevska, O., Nedelkov, D., 2011. PLoS One 6 (e17282), 1–8.
Lee, N.S., Kim, H.S., Park, S.E., Blüher, M., Park, C.Y., Youn, B.S., 2018. Sci. Rep. 8, 6–11.
Lee, S., Zhang, C., Kilicarslan, M., Piening, B.D., Bjornson, E., Hallström, B.M., Groen, A.K., Ferrannini, E., Laakso, M., Snyder, M., Blüher, M., Uhlen, M., Nielsen, J., Smith, U., Serlie, M.J., Boren, J., Mardinoglu, A., 2016. Cell Metab. 24, 172–184.
Lee, S.J., Park, J.W., Kim, I.A., Youn, B.S., Gu, M.B., 2012. Sens. Actuators B Chem. 168, 243–248.
Lee, S.J., Youn, B.-S., Park, J.W., Niazi, J.H., Kim, Y.S., Gu, M.B., 2008. Anal. Chem. 80, 2867–2873.
Li, L., Chen, S., Jiang, S., 2007. J. Biomater. Sci. Polym. Ed. 18, 1415–1427.
Mahmood, T., Yang, P.C., 2012. N. Am. J. Med. Sci. 4, 429–434.
Mostafalou, S., Eghbal, M.A., Nili-Ahmadabadi, A., Baeeri, M., Abdollahi, M., 2012. Toxicol. Ind. Health 28, 840–851.
Narayan, K.M.V., Chan, J., Mohan, V., K.M.V, N, J., C, V., M, 2011. Diabetes Care 34, 244–246.
Nichols, G.A., Bell, K., Kimes, T.M., O'Keeffe-Rosetti, M., 2016. Diabetes Care 39, 1981–1986.
Nuzzo, R.G., Allara, D.L., 1983. J. Am. Chem. Soc. 105, 4481–4483.
Okafor, C., Grooms, D., Alocilja, E., Bolin, S., 2014. Sensors 14, 19128–19137.
Pakzad, M., Fouladdel, S., Nili-Ahmadabadi, A., Pourkhalili, N., Baeeri, M., Azizi, E., Sabzevari, O., Ostad, S.N., Abdollahi, M., 2013. Pestic. Biochem. Physiol. 105, 57–61.
Parkash, O., Shueb, R.H., 2015. Viruses 7, 5410–5427.
Patil, B., Kobayashi, Y., Fujikawa, S., Okajima, T., Mao, L., Ohsaka, T., 2014. Bioelectrochemistry 95, 15–22.
Perween, M., Parmar, D.B., Bhadu, G.R., Srivastava, D.N., 2014. Analyst 139, 5919–5926.
Perween, M., Srivastava, D.N., 2017. Chem. Select 2 (16), 4428–4432.
Rahimi, R., Nikfar, S., Larijani, B., Abdollahi, M., 2005. Biomed. Pharmacother. 59, 365–373.
Sonuç, M.N., Sezgintürk, M.K., 2014. Talanta 120, 355–361.
Stevens, T.E., Pearce, C.J., Whitten, C.N., Grant, R.P., Monson, T.C., 2017. Sci. Rep. 7, 39–44.
Tabatabaei-Malazy, O., Larijani, B., Abdollahi, M., 2013. J. Med. Hypotheses Ideas 7, 25–30.
Tabatabaei-Malazy, O., Nikfar, S., Larijani, B., Abdollahi, M., 2016. Expert Opin. Pharmacother. 17, 2449–2460.
Vakhshiteh, F., Allaudin, Z.N., Mohd Lila, M.A.B., Hani, H., 2013. Xenotransplantation 20, 82–88.
Walker, J.M., Rapley, R., 2008. Molecular Biomethods Handbook, 2nd ed. .
Wen, J., Tian, Z., Ma, J., 2013. J. Phys. Chem. C 117, 19934–19944.
Yang, Q., Graham, T.E., Mody, N., Preitner, F., Peroni, O.D., Zabolotny, J.M., Kotani, K., Quadro, L., Kahn, B.B., 2005. Nature 436, 356–362.